Proton-Transfer Reaction of 4-Methyl 2,6-Diformyl Phenol in Cyclodextrin Nanocage

Madhuri Mukhopadhyay,[†] Debi Banerjee,[‡] and Samaresh Mukherjee*[,†]

Department of Physical Chemistry, Indian Association for the Cultivation of Science, Jadavpur, India, and Department of Physics, Shibpur Dinabandhu Institution (College), Shibpur, Howrah, India

Received: June 15, 2006; In Final Form: September 27, 2006

We report here on the steady-state and time-resolved fluorescence studies on proton-transfer (PT) reaction of 4-methyl 2,6-diformyl phenol (MFOH) in confined nanocavities in three solvents, dimethyl sulfoxide (DMSO), dimethyl formamide (DMF), and water. Though DMSO and DMF individually interact with MFOH in a similar fashion, their modes of interaction get significantly modified in the presence of cyclodextrin (CD) nanocages. In DMSO, in the ground state, the solvated molecular anion of MFOH forms 1:1 inclusion complex with β- or γ-CD and attains greater stability compared to the normal form. In DMF, the solvated molecular anion gets converted to the H-bonded complex within the CD cavity resulting in a 50-nm blue shift in the absorption spectra. In the excited state, the anionic species gets more stabilized in DMSO while in DMF it is significantly destabilized in the presence of CDs. However, in case of water, MFOH gets trapped inside the water cages so that the CDs fail to complex with it effectively. There are also no changes in the excited-state lifetimes in water in the presence of CDs, but in case of DMSO and DMF, because of restricted rotation of the formyl group within the CD cavity, the contribution of the shorter lifetime components reduce significantly increasing the larger components. Some theoretical calculations at the AM1 level of approximation have also been carried out to demonstrate how the dipolar nature of the solvent influences excited-state PT in confined media.

1. Introduction

It is well established that the driving force for proton-transfer (PT) reaction is the redistribution of charges in the excited state with respect to the ground state.[1−3] Hence, it can be said that the microenvironment around the proton and the changes occurring in it influence the PT reaction. A good number of earlier works have been carried out to recognize the immense influence of solvents on PT reactions.[4,5] Changes in the dielectric properties[6−8] and in the electron-donating and H-bonding abilities[9−12] of the solvents are the major factors affecting PT reaction. It has also been established that not only the electrostatic environment but also confinement effects play an important role toward modulating the excited-state proton-transfer (ESPT) processes.[13−17] Several studies on ESPT in cyclodextrin nanocavities[18−25] or micellar media[26−31] have been reported.

4-Methyl 2,6-diformyl phenol (MFOH) is a well-studied PT probe[32−36] and effects of different solvent environments on it have extensively been studied.[37,38] However, the effect of cyclodextrin cavities on PT reaction of MFOH has not yet been observed. The present study aims to investigate how different highly polar solvents such as dimethyl sulfoxide (DMSO) and dimethyl formamide (DMF) in conjunction with the probe within the cyclodextrin (CD) cavity affect the PT reaction in case of MFOH, while the CD nanocavities on their own do not produce any substantial effect on PT. Moreover, the central issue of this study is that although pure solvents such as DMSO and DMF individually exhibit a similar type of character and regulate PT reaction of MFOH in an almost similar fashion,[39−41] the behavior of these two solvents is significantly different in the interior of the CD cage and hence affect the PT reaction in completely different ways. The inclusion of guest molecules into the cavities of supramolecular hosts with molecular container properties has the potential to allow the novel chemical transformation to isolate reactive species, to mimic enzymatic activity, and to promote uncommon spectroscopic effects.[42−47] The cyclodextrin nanocages are good tools to explore or control the spectroscopy (space domain) and dynamics (time domain) of chemical or physical changes in real time.[13−17] The hydrophobic interior and hydrophilic exterior of these molecular pockets make them suitable and fascinating hosts for PT probes. The reduced degrees of freedom of the guest molecules in the cavity offer a unique opportunity to study the PT reaction in a totally different electrostatic and steric environment compared to the bulk solvents. The rate of deprotonation of β-CD bound carbazole[48] and protonated 1-aminopyrene[20] has been found to be higher than that of the corresponding free molecules while a decrease of deprotonation rate has been observed for naphthols.[49] In case of salicylidine 3,4,7-methylamine, the excited-state intermolecular PT is highly perturbed in the presence of CD solutions.[14] Hansen et al.[20] probed the water environment of cyclodextrin to measure the rate of excited-state proton transfer of the inclusion complexes of 1-amino pyrine and 1-naphthol. They proposed that the extent of the effects depend on the dimensions of the CD cavity and on the structure and the stoichiometry of the inclusion complex. Also, the major interaction within the CD cavity is noncovalent in nature.

In the present paper, fluorescence properties and time-resolved laser spectroscopy have been used as tools to describe the moderating role of DMSO and DMF on PT of MFOH in CD nanocavities. With the help of some theoretical calculations at

* Author to whom correspondence should be addressed. Tel: +91-33-2473-4971. Fax: (91) 33-2473-2805. E-mail: pcsm@mahendra.iacs.res.in.
[†] Indian Association for the Cultivation of Science.
[‡] Shibpur Dinabandhu Institution (College).

10.1021/jp063724r CCC: $33.50
Published on Web 11/07/2006

SCHEME 1

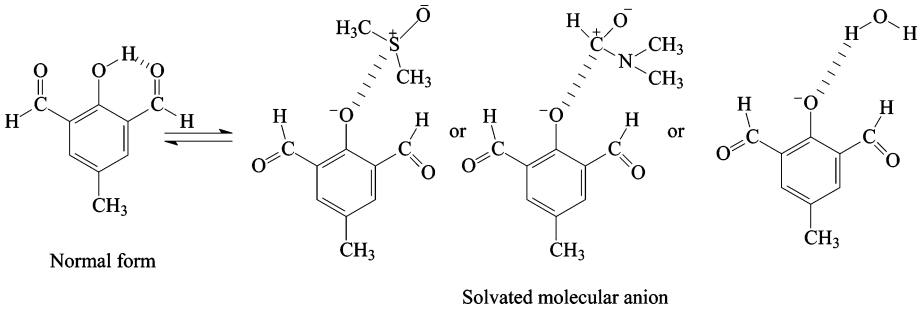

the AM1 level of approximation, it has also been shown how the dipolar nature of the solvents becomes the critical parameter to perturb the ESPT in confined environments.

2. Experimental Section

2.1. Materials and Solutions. MFOH was prepared in the inorganic chemistry department of this institute in a similar way to that reported earlier.[33] The compound was recrystallized from methanol and was dried before use. The solvents, dimethylsulfoxide (DMSO) and dimethyl formamide (DMF), were of spectroscopic grade (Aldrich or Merck) and were checked for residual fluorescence before use. Triply distilled water was used throughout. AR grade cyclodextrins (α-, β-, and γ-) from Fluka have been used as nanocages. The concentration of MFOH was maintained at $\sim 1 \times 10^{-6}-5 \times 10^{-5}$ mol dm^{-3}, and the concentration of CDs was varied as required ([CD] $\sim$ 0−14 mM). The solutions were all freshly prepared. Since the fluorescence quenching by dissolved oxygen was unimportant, the fluorescence measurements were made with nondegassed solution. All the experiments were performed at ambient temperature (23 °C).

2.2. Instruments. The room-temperature absorption and emission spectra were recorded on a Shimadzu UV−Vis Recording Spectrophotometer, UV-2401 (PC) S220V and Fluoro Max 3 (Jobin Yvon Horiba) fluorimeter, respectively. In all cases, 1-cm path length quartz cell was used. For lifetime measurements, the sample was excited at 375 nm using a picosecond diode laser (IBH Nanoled - 07) in an IBH Fluorocube apparatus. The emission was collected at a magic-angle polarization using a Hamamatsu MCP photomultiplier (5000U - 09) on the basis of time-correlated single-photon-counting (TCSPC) technique. The TCSPC setup consists of an ortic 9327 CFD and a Tennelec TC 863 TAC. The data were collected with a PCA3 card (Oxford) as a multichannel analyzer. The typical fwhm of the system response using a liquid scatterer was about 80 ps. The fluorescence decays were deconvoluted using IBH DAS6 software.

3. Results

3.1. Steady-State Absorption and Emission Spectra in Pure Solvents. It has been reported in our earlier work that in the ground state, MFOH ([MFOH] $\sim 10^{-5}$ M) exhibits two different molecular forms, intramolecularly H-bonded normal form and the solvated molecular anion in dilute solutions in DMSO, pure water, and DMF (Scheme 1).[33,36] The observed absorption maximum ($\lambda_{max} = 352$ nm) is attributed to the normal form in all the three solvents. The absorption maximum resulting from the anion absorption is highly dependent on the nature of the solvent used and appears at 430 nm in water and peaks around 490 nm in DMSO and DMF. It is also observed that the absorption spectra are dependent on the concentration of MFOH. At very low concentration of MFOH ($\sim 10^{-6}$ M) in DMF, only the 490-nm peak exists whereas at higher concentration (5×10^{-5} M), MFOH shows both peaks. When excited at 352 nm, MFOH exhibits dual emission at 460 and 520 nm in DMSO and DMF and a single peak at 520 nm in water. However, on excitation at 490 nm, a single peak appears at 520 nm in all the three cases. The 460- and 520-nm emission bands have been assigned to H-bonded complex and anion of MFOH as reported previously.[33−36]

3.2. Steady-State Absorption and Emission Spectra in the Presence of Cyclodextrins. On addition of α-CD to a DMSO solution of MFOH, no significant spectral change is observed both in the ground as well as in the excited state (Figure 1and inset). However, on addition of β- or γ-CD, the 352-nm peak decreases with a simultaneous increase of the 490-nm peak in the ground state (Figure 2), and an isosbestic point is observed at 380 nm in both cases, indicating the presence of equilibrium between the two species. To analyze the situation and to obtain ground-state association constant (K_g) for MFOH−CD inclusion complex, we have used the Benesi−Hildebrand (B−H) linear regression analysis. The method provides reliable information on the stoichiometry of the complex.[14] The B−H analysis for 1:1 stoichiometry is given by eq 1

$$\frac{1}{I - I_0} = \frac{1}{I_1 - I_0} + \frac{1}{(I_1 - I_0)K_g}\frac{1}{[\mathrm{CD}]} \qquad (1)$$

where I_0 = initial absorbance of free guest, I_1 = absorbance of guest−host complex, I = observed absorbance of guest and guest−host mixture, and K_g = ground-state association constant for the 1:1 complex formation.

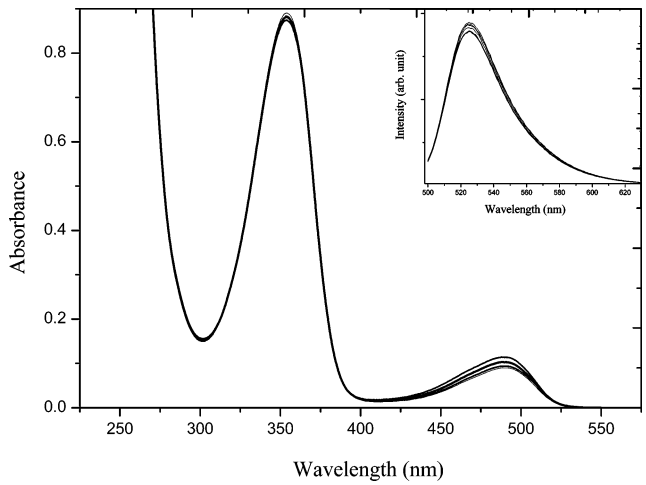

Figure 1. Absorption spectra of MFOH in DMSO in the presence of α-CD, inset shows the corresponding emission spectra ($\lambda_{exc} = 490$ nm). Range of [α-CD] = 0−14 mM.

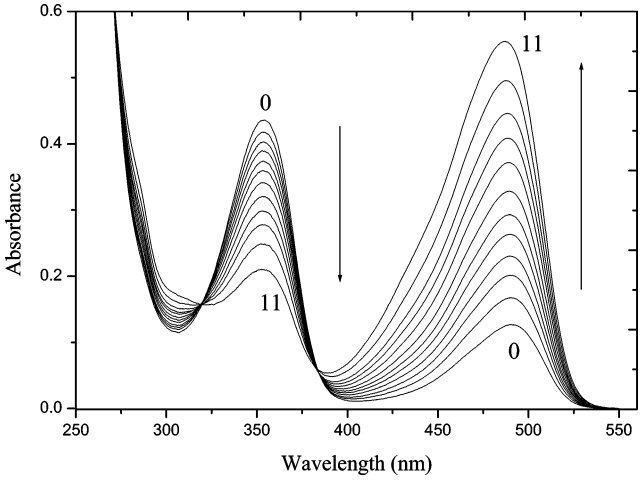

Figure 2. Absorption spectra of MFOH in DMSO in the presence of γ-CD. Range of [γ-CD] = 0−14 mM.

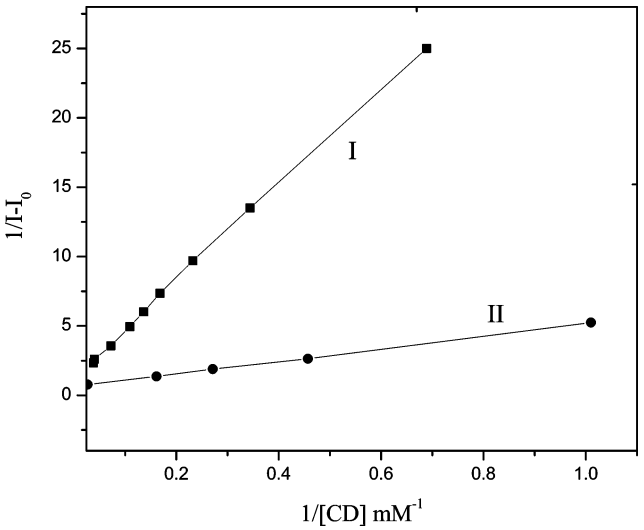

Figure 3. Benesi−Hildebrand plot for MFOH complexed to β-CD (I) and γ-CD (II), assuming 1:1 MFOH−CD complex in DMSO.

The observed data satisfy eq 1 giving rise to a linear plot as shown in Figure 3 that is, the linear B−H plot indicates that the ground-state inclusion complex has a 1:1 stoichiometry. The K_g values obtained from the slope and intercept of the plots are 13.0/M^{-1} for β-CD (with a standard deviation of the linear fit being 0.521) and 33.0/M^{-1} for γ-CD (with a standard deviation of the linear fit being 0.253). In the excited state, on addition of β- or γ-CD, the 460-nm peak increases at the expense of the 520-nm peak with the appearance of isoemissive point, when excited at 352 nm (Figure 4). However, when excited at 490 nm, the 520-nm emission intensity continuously increases with an increase of β- or γ-CD concentration (Figure 5). In presence of glucose, no significant change is observed both in the ground as well as in the excited state.

Although for the DMF solution of MFOH, the observed spectra are similar to those observed in DMSO, interestingly, the spectral changes of MFOH in DMF, in the presence of the three different CDs individually, are quite different to those observed in DMSO solution. In DMSO solution, while α-CD does not interact effectively with MFOH, in DMF, it affects the system significantly. In the ground state, when α-CD is added to a dilute solution of MFOH in DMF ($\sim 10^{-6}$ M), the 490-nm peak gets shifted to the 440-nm region. This shift

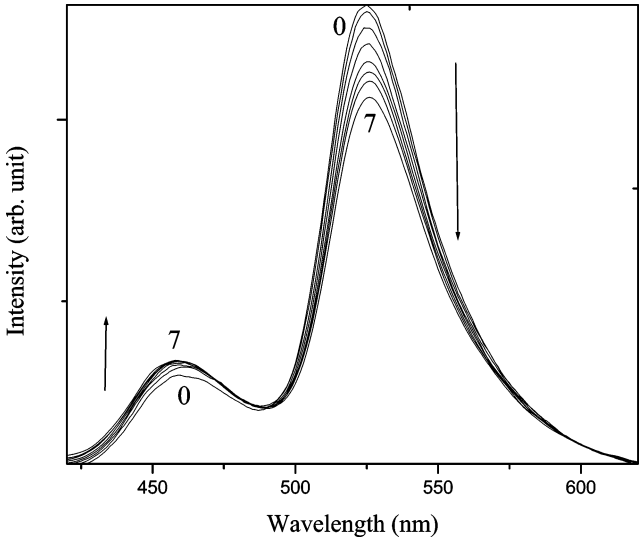

Figure 4. Fluorescence spectra of MFOH in DMSO in the presence of β-CD, λ_{exc} = 350 nm. Range of [β-CD] = 0−14 mM.

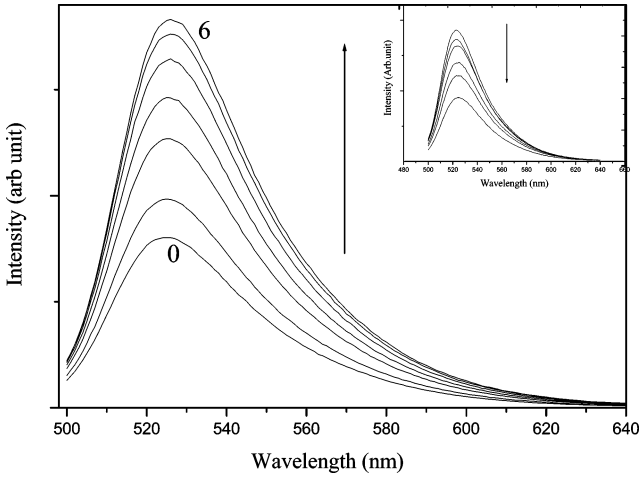

Figure 5. Fluorescence spectra of MFOH in DMSO in the presence of γ-CD, λ_{exc} = 490 nm. Range of [γ-CD] = 0−14 mM. Inset shows fluorescence spectra of MFOH in DMF in the presence of β-CD, λ_{exc} = 490 nm. Range of [β-CD] = 0−14 mM.

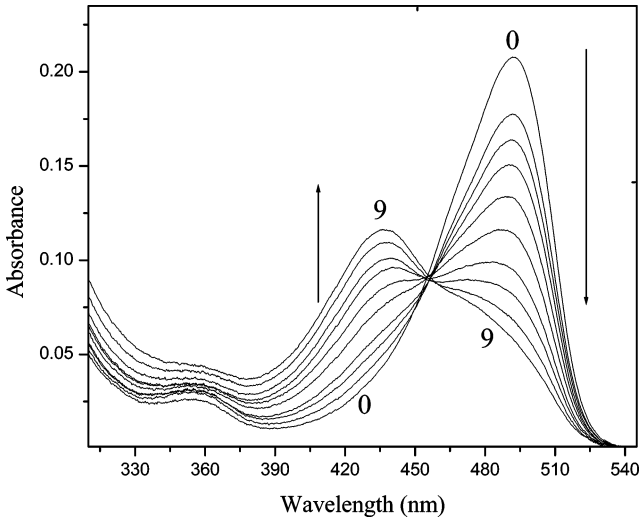

Figure 6. Absorption spectra of MFOH in DMF in the presence of γ-CD. Range of [β-CD] = 0−14 mM.

becomes more prominent when β- or γ-CD is added instead (Figure 6). The B−H plot of the ground-state data for a DMF solution in the presence of either of the CDs shows deviations

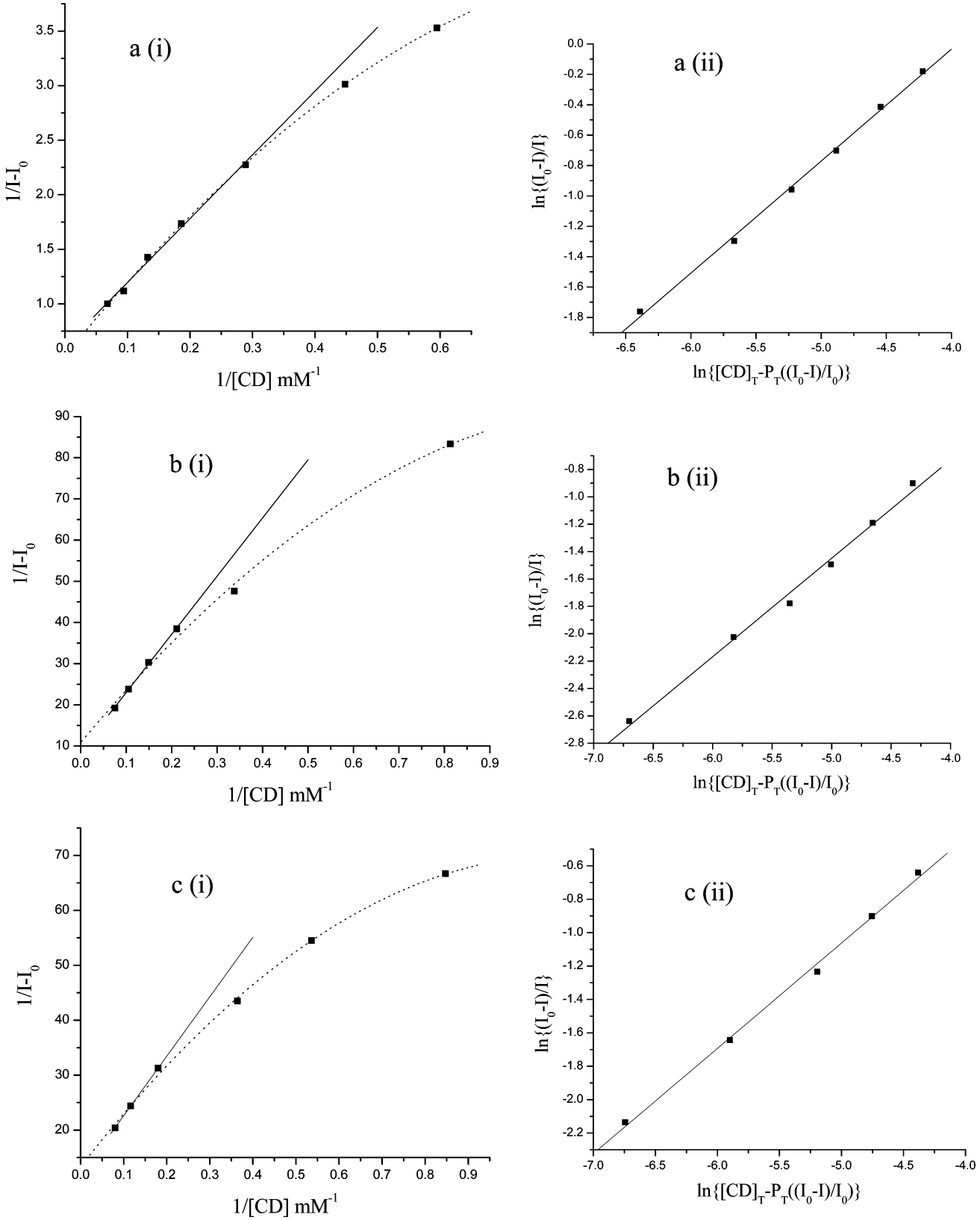

Figure 7. Benesi−Hildebrand plots for MFOH complexed to α-CD (a (i)), *β*-CD (b (i)), and *γ*-CD (c (i)), in DMF, showing deviation from linearity for 1:1 complex. The plots a (ii), b (ii), and c (ii) depict the fitting to the appropriate stoichiometry for MFOH complexed to α-CD, *β*-CD, and *γ*-CD, respectively.

from linearity for 1:1 complex (Figure 7). Considering a reactionof the form $P + n[CD] \rightarrow P[CD]_n$, where P is the probe (guest) MFOH, $P[CD]_n$ is the complex formed, and n is the number of CD molecules complexating with one MFOH molecule, we can obtain the ground-state association constant, K_g in this case using eq 2[50]

$$\ln\left(\frac{I_0 - I}{I}\right) = \ln K_g + n \ln\left\{[CD]_T - P_T\left(\frac{I_0 - I}{I_0}\right)\right\} \quad (2)$$

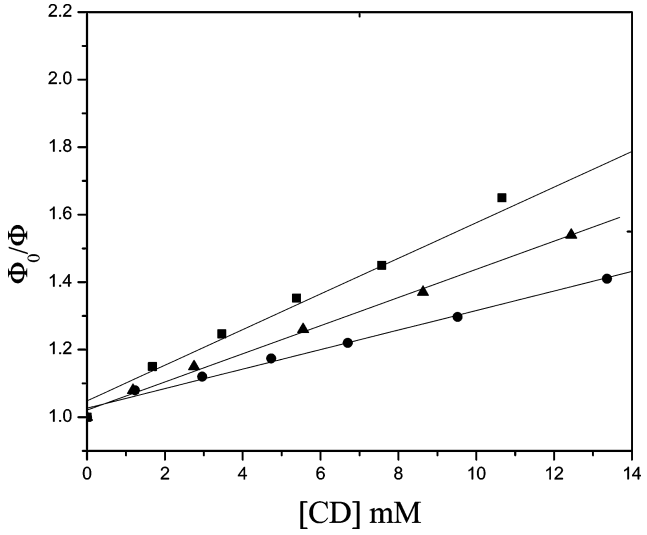

Figure 8. Stern−Volmer plots for the quenching of MFOH anion in DMF by α-(■), *β*-(●), and *γ*-(▲)CD.

where I_0 = initial absorbance of free guest, I = observed absorbance of guest after complexation, K_g = ground-state association constant for the 1:*n* complex formation, n = number of CD molecules complexating with one probe molecule, P_T = total concentration of the probe molecule, and $[CD]_T$ = total concentration of CD molecule.

From the plot of $\ln((I_0 - I)/I)$ versus $\ln\{[CD]_T - P_T((I_0 - I)/I_0)\}$ (Figure 7), the number *n* is obtained to be 0.74, 0.72, and 0.63 in case of interaction of MFOH with α-, *β*-, and *γ*-CD, respectively. The values of "*n*" so obtained also reflect the fact that because the cavity size of *γ*-CD is the greatest while that of α-CD is the smallest a lesser fraction of *γ*-CD molecules would be required to encapsulate one MFOH molecule followed by *β*-CD and α-CD in that order. Also, from the B−H plots in case of DMF, it was observed that the deviation from linearity occurred in the region of a lower CD concentration while the 1:1 complexation was evident at higher CD concentrations supporting the fractional values of *n* obtained in the three cases.

In the excited state, when the DMF solution of MFOH with the different CDs are excited at 352 nm, the dual emission at 460 and 520 nm increase simultaneously in all the cases, in contrast to DMSO, where the 460-nm peak increases at the expense of the 520-nm peak. When the excitation is done at 490 nm, the single emission peak at 520 nm is significantly quenched in all the three cases (Figure 5, inset), whereas the trend totally reverses in DMSO, that is, the single emission peak increases with the addition of CDs. The bimolecular quenching constant (k_q) of MFOH in DMF by the added CDs obtained from the linear Stern−Volmer plots (Figure 8) are 1.23×10^{10}, 7.07×10^9, and 1.02×10^{10} dm^3 mol^{-1} s^{-1} for α-CD, *β*-CD, and *γ*-CD, respectively. On the addition of glucose to the DMF solution of MFOH, there is no significant spectral change. In aqueous solution of MFOH, no significant spectral changes are observed both in the ground and the excited state.

3.3. Time-Resolved Measurements. In DMSO and DMF, MFOH shows biexponential decay at both 460 and 520 nm (Table 1). It has been shown in earlier studies on MFOH at the nanosecond time scale[33−36] that both the H-bonded complex and anionic emission could be represented by a monoexponential decay with a lifetime of 3.9 and 4.1 ns, respectively, in DMF. This agrees fairly well with the longest decay components of 3950 and 4090 ps obtained in the present study (λ_{mon}= 460 and 520 nm, respectively), and hence these components can be attributed to H-bonded complex and the anionic emission. Table 1 shows that when α-CD has been added to the MFOH solution in DMSO, there are no significant changes in the values of the lifetime components as well as in the percent contributions, which also support the steady-state observations. On the addition of *β*- or *γ*-CD, there are no significant changes in the lifetime values at both the wavelengths, but the relative amplitudes of the long-lived component at both the wavelengths are found to increase with a simultaneous decrease of the shorter components (Figure 9). In case of DMF solution, the addition of different CDs cause increase in amplitude for both the 520- and 460-nm emissions for the long-lived component (Table 1). In water, MFOH shows biexponential decay when it is monitored at 525 nm. The lifetime components as well as amplitudes of the species remain more or less constant on addition of all the different CDs in water.

TABLE 1: Lifetime Components of MFOH in Different Solvents, in Absence and Presence of α-, *β*-, and *γ*-CD (λ_{exc} = 375 nm)[a]

	λ_{mon} = 460 nm (for DMSO & DMF)		λ_{mon} = 525 nm (for water), = 520 nm (for DMSO & DMF)	
MFOH+	τ_1 (ps)	τ_2 (ps)	τ_1 (ps)	τ_2 (ps)
water			650 (31.15)	4830 (68.85)
water + α-CD			620 (30.96)	4830 (69.04)
water + *β*-CD			630 (29.59)	4910 (70.40)
water + *γ*-CD			620 (30.71)	4900 (69.28)
DMSO	40 (73.35)	4380 (26.64)	550 (7.05)	4110 (92.95)
DMSO + α-CD	50 (73.65)	4370 (26.34)	240 (17.56)	4080 (82.43)
DMSO + *β*-CD	50 (69.75)	4300 (30.25)	430 (12.23)	4150 (87.76)
DMSO + *γ*-CD	50 (64.00)	4260 (36.00)	480 (10.85)	4150 (89.15)
DMF	550 (31.82)	3950 (68.18)	500 (62.86)	4090 (37.14)
DMF + α-CD	500 (47.48)	3930 (52.52)	380 (60.91)	4260 (39.09)
DMF + *β*-CD	660 (37.45)	3940 (62.55)	410 (54.50)	4210 (45.50)
DMF + *γ*-CD	590 (31.94)	3860 (68.06)	360 (48.56)	4300 (51.44)

[a] The percent contributions of the corresponding lifetimes are shown in parenthesis. The χ^2 values range from 0.99 to 1.20. In all the above cases, 8 mM CD concentration is maintained.

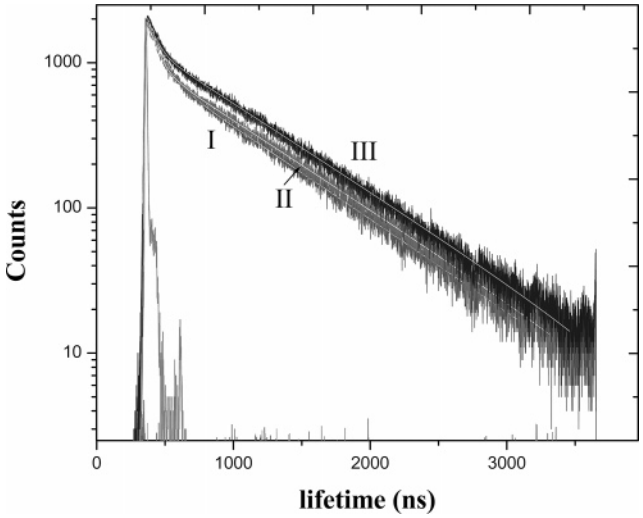

Figure 9. Typical decay profile of MFOH in DMSO (I), in the presence of *β*-(II), and *γ*-(III) CD. Global analysis of the decay and the lamp profile is also shown.

4. Discussion

A solvent should not be considered as a macroscopic continuum characterized only by physical constants but as a discontinuum, which consists of individual, mutually interacting solvent molecules. According to these interactions, some solvent remains with a pronounced internal structure in dynamical

SCHEME 2

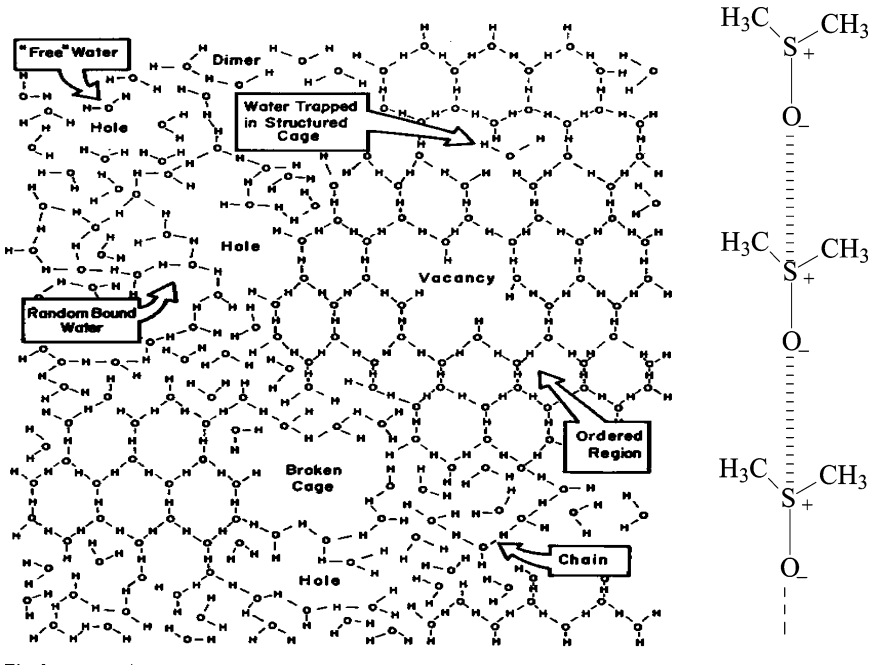

TABLE 2: Properties of Solvents as Obtained from AM1 Calculation and Kamlet−Taft Parameters

solvents	charge (Mulliken unit)	atom electron density (Mulliken unit)	dipole moments (*D*)	π^*	a	b
water	O(1) = −0.38	6.38	1.86	0.52	0.78	0.00
DMSO	S(1) = 1.39	4.60	3.96	1.00	0.00	0.76
	O(2) = −0.78	6.77				
DMF	C (1) =0.26	3.74	3.82	0.88	0.00	0.69
	O(2) = −0.36	6.36				

equilibrium, say, an ordered structure like a cage or a chain or randomly bound and free solvents (Scheme 2).

In general, it can be said that the greater the dielectric constants, greater are the varieties of interactions. As a result, the cagelike structure is very common in water (dielectric constant, $\epsilon = 80.2$, dipole moment = 1.84 D), whereas in bulk DMSO ($\epsilon = 46.7$, dipole moment = 3.96 D) most of the molecules remain in the chain form (Scheme 2), compared to that in DMF ($\epsilon = 36.7$, dipole moment = 3.82 D). Because of the highly dissociating nature of the abovementioned solvents, the anion is formed in addition to the normal form of MFOH in the ground state.[33,36] The AM1 dipole moment and charge density as well as electron density calculations for individual molecules of the solvents in the ground state are shown in Table 2. The dipole moment of the normal and the anionic form of MFOH is shown in Table 3. From Table 2, DMSO and DMF are seen to be more polar than water and hence are expected to stabilize MFOH anion more compared to water (Scheme 3). This also agrees well with our experimental observations on the absorption spectra, where the anion appears to be more blue-shifted in water compared to the other two solvents. The close values of the dipole moments of DMSO and DMF support the similar type of observations obtained in these two solvents.

When CD is added to the aqueous solution of MFOH, there are no changes in the ground- and excited-state spectra indicating

TABLE 3: Properties of MFOH Obtained from AM1 Calculations and the Optimized Geometry of the Excited-State Anion with the Values of Different Distances

different conformers of MFOH	charge (Mulliken unit)	atom electron density (Mulliken unit)	dipole moments (*D*)
normal form (GS)	O(1) = −0.26	6.21	2.47
	H(2) = 0.12	0.92	
anion (GS)	O(1) = −0.473	6.47	5.73
anion (ES)	O(1) = −0.37	6.37	5.67

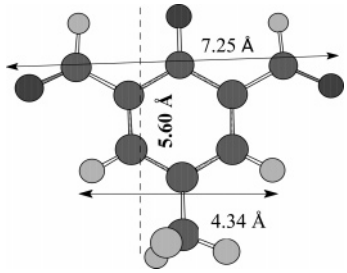

SCHEME 3

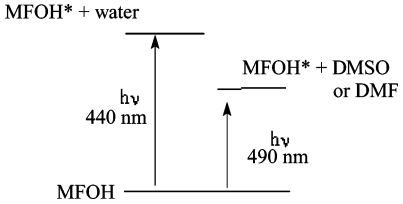

almost no change in the microenvironment of both the normal and the anionic forms of MFOH. In other words, the MFOH normal form and the anion are effectively trapped in the cagelike structure of water. Moreover, the interior of the CD nanocage being hydrophobic, probably no water molecule prefers to enter

SCHEME 4

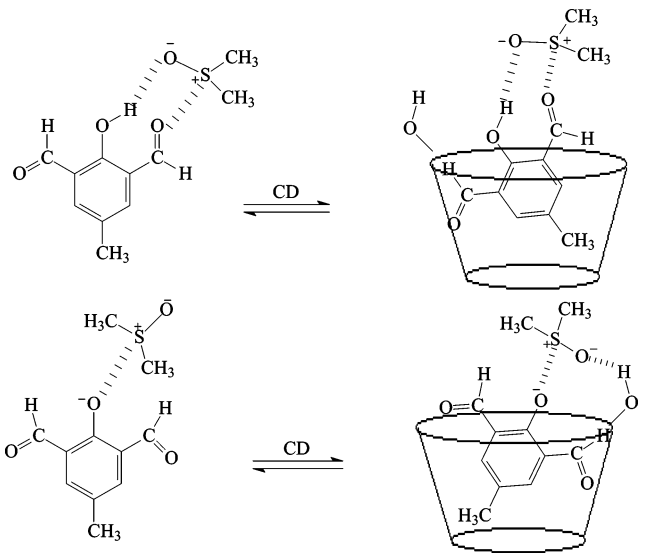

the CD cavity. Hence, none of the solvated MFOH molecules effectively enter into the cavity thereby resulting in no new interactions.

In the liquid state, DMSO seems to assume a chainlike structure held together by the dipolar interaction of sulfur and oxygen (as shown in Scheme 2), and hence it has the ability to associate with ionic molecules (valence electron density on the anionic oxygen atom of MFOH is 6.37). Table 2 depicts that the charge on the sulfur atom of DMSO is sufficiently positive (+1.39) to stabilize an anionic species and the valence electron density on the oxygen atom is sufficiently high (6.77) to accept a proton forming a strong H-bond (Scheme 4). Though the CD cavity is highly hydrophobic, the hydrogen atoms of the hydroxyl groups at the rim of the CD cavity can form strong H-bond with the DMSO oxygen (Scheme 4).

Although DMF and DMSO have similar dielectric constants and dipole moments reflecting similar solvent properties, Table 2 reveals that the $\delta+$ character of C atom in DMF is much less than $\delta+$ character of S atom in DMSO. Also, the electron density on the O atom in DMF is less than that on the O atom in DMSO. This imparts a better H-bonding ability to DMSO in comparison to DMF. Also, from the Kamlet−Taft parameters[51] (Table 2), it is seen that the index of solvent polarizibility (π^*) of DMSO is very high (1.00) and also greater than DMF (0.88) and the H-bond accepting ability (β) of DMSO (0.76) is also greater than DMF (0.69). Thus, it is expected that DMSO can enter into H-bonding interaction with the hydroxyl group at the rim of the CD cavity and also simultaneously stabilize the MFOH anion through dipolar interaction (Scheme 4) but not DMF.

CDs being naturally occurring cyclic oligosaccharides consisting of at least six glucosyl residues,[52] it is expected that their electronic character will be somewhat similar to that of glucose. As mentioned earlier, in the presence of glucose there are no significant changes indicating that the cagelike structure of CD is the most vital factor regulating the interactions. Again, when α-CD is added to the DMSO solution of MFOH, no observable change results, compared to β- and γ-CD, reflecting that the cage size of α-CD may not be sufficient to interact with MFOH. However, spectral changes do occur when α-CD is added to the DMF solution of MFOH. Hence, it can be argued that not only the size of the CD cavity but also the nature of the solvent plays a crucial role in the observed interactions. To get a clearer picture regarding partial encapsulation of MFOH within the α-CD cavity, we have done some quantum mechanical calculations at the AM1 level. The optimized geometry of MFOH is shown below Table 3, where the different end-to-end distances have been denoted, while the relevant physical parameters are shown in Table 3. It is clear from the data that from the methyl group side of MFOH (where the maximum end-to-end distance is 4.34 Å, as shown in the optimized geometry), MFOH can enter partially into the α-CD cage (the diameter of α-CD being 4.5 Å). It has been proposed in Scheme 4 that solvent-mediated interaction occurs between MFOH and CD in the presence of DMSO, which is possible due to a large electron density on the O atom and a high positive charge on the S atom (Table 2). However, in case of DMF, both the electron density on the O atom and the electropositive character of the C atom are insufficient to warrant such a solvent-mediated interaction between the CD and MFOH. As shown in Scheme 5, in the DMF solution, the CDs interact directly with MFOH via H-bonding through its hydroxyl group projected at the rim of the CD cavity. This explanation is also supported by the spectral shift observed in DMF in the presence of CD which is absent in DMSO thereby reflecting that solvation energy is changed

SCHEME 5

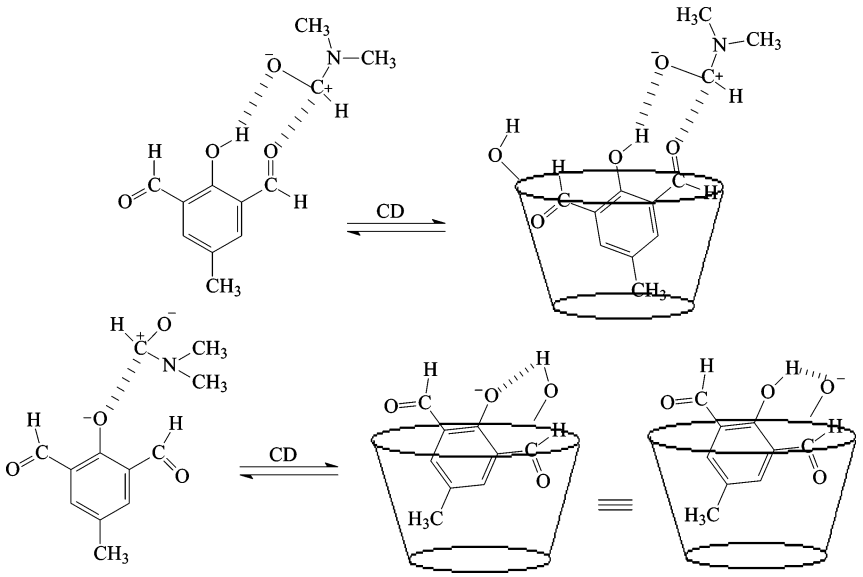

in the DMF solution in the presence of CD, which is due to a drastic change in the environment of the anion. Again, the shift to 440 nm because of H-bonding between the hydroxyl group of CD and MFOH anion is also supported by a previous observation,[36] which shows that in the presence of ethanol, the MFOH anion appears in the 440-nm region. Thus, in the DMF solution of MFOH, MFOH enters partially into the α-CD cavity alone producing a H-bonding interaction as shown in Scheme 5.

Next, we try to analyze whether the proposed schemes are also adequate to interpret the excited-state observations. The enhancement of the anionic emission of MFOH at 520 nm (λ_{exc}= 490 nm) in DMSO without any spectral shift reflects that some of the nonradiative rates have been quenched enhancing the radiative decay without any change in the solvation. Now from Scheme 4, it is evident that as the CH_3 group and the benzene ring of MFOH get incorporated into the CD cavity, the vibrational degrees of freedom, especially, the out-of-plane bending modes, get restricted. Thus, it can be said that owing to this confinement, the nonradiative rates reduce leading to an enhancement in the anionic emission.

It is already mentioned that the 352-nm excitation favors the intermolecular H-bond formation with oxygen, an observation also seen in the presence of CD, as shown in Scheme 4. The H-bonded complex in DMSO in the excited state is preferred over the anion in the presence of CDs (on excitation at 352 nm), which is reflected by the increase of the 460-nm emission at the expense of the 520-nm emission (Figure 4).

In the presence of DMF, on exciting at 352 nm, both the 460- and 520-nm peaks increase simultaneously, which can be rationalized from Scheme 5. The scheme reflects that both the normal form and the anion of MFOH enter into H-bonding with the hydroxyl groups at the rim of the CD cavity, although via slightly different interactions. Further, it may be proposed that the quenching of the anionic emission in DMF in the presence of CD may be due to the formation of the H-bonded complex.

In the DMSO solution, the solvent gets incorporated into the CD cavity along with MFOH but in case of DMF, the interactions are mainly directly with the CD. The incorporation of MFOH within the CDs is further supported by the time-resolved measurements. From these measurements, the shorter lifetime components may be argued to be due to the rotation of the formyl group of MFOH. It has been found that the amplitude of the shorter components reduces significantly in those cases where MFOH enters within the CD cavities. Because of the encaging of MFOH by the CD cavity, the formyl group experiences a restricted rotation resulting in a decrease of the shorter decay components. Thus, in the presence of all the three CDs in water and in the presence of α-CD in DMSO, there is no change in the contribution of the shorter components.

5. Conclusion

In the present study, we focus our attention on the changes in solvent interactions resulting because of the incorporation of MFOH within the CD nanocavity. It is found that MFOH prefers to remain in the water cage rather than enter into the CD cavity while DMSO enters within the CD cage along with MFOH. It has been found that the interaction between DMSO and MFOH molecules remains the same both in the bulk solvent as well as inside the CD cavity. However, in case of DMF, MFOH enters into interaction directly with CD instead of the solvent. In DMF, the change in interaction from bulk solvent to CD cavity is manifested through the spectral shift, which may be due to a change in solvation energy. Though pure DMSO and DMF individually interact with MFOH in a similar fashion, the difference of electron density on the donor O atoms and the $\delta+$ character of S and C atoms of DMSO and DMF, respectively, introduce different interactions with the CDs. The B−H plot shows that in DMSO, MFOH forms 1:1 complex with β- and γ-CD in the ground state. In DMF, the B−H plots are deviated from linearity for 1:1 complex, and the data instead depict a 1:*n* complex where *n* is a fractional number. The time-resolved studies show that in those cases where MFOH enters within the CD cage, the contribution of the shorter lifetime components gets significantly reduced because of the restricted rotation of the formyl group of MFOH.

Acknowledgment. We thank the Department of Inorganic Chemistry, IACS for the compound MFOH. We thank Professor K. Bhattacharyya of this department for allowing us to measure the decay times in the picosecond time scale. We would like to acknowledge DST project no. IR/I-1/CF-01/2002 in this context. M.M. is grateful to CSIR for providing her with a senior research fellowship. M.M. and D.B. would also like to thank Dr. Sivaprasad Mitra and Ms. Durba Roy for various suggestions and discussions.

References and Notes

(1) Agmon, N. *J. Phys. Chem. A* **2005**, *109*, 13−35.
(2) Scheiner, S. *J. Phys. Chem. A* **2000**, *104*, 5898−5909.
(3) Sakota, K.; Sekiya, H. *J. Phys. Chem. A* **2005**, *109*, 2718−2721.
(4) Mandal, A.; Nath, D. N.; Mukherjee, S.; Mitra, S.; Das, R. *J. Chem. Phys.* **2002**, *117*, 5280−5289.
(5) McMorrow, D.; Aartsma, T. J. *Chem. Phys. Lett.* **1986**, *125*, 581−585.
(6) *Hand book of Solvents*; Wyspych, G., Ed.; William Andrew: New York and Chem Tec Publishing: Toronto, 2001.
(7) Brucker, G. A.; Swinney, T. C.; Kelley, D. F. *J. Phys. Chem.* **1991**, *95*, 3190−3195.
(8) Chou, P. T.; Martinez, M. L.; Clements, J. H. *J. Phys. Chem.* **1993**, *97*, 2618−2622.
(9) Verner, M. V.; Scheiner, S. *J. Phys. Chem.* **1995**, *99*, 642−649.
(10) Scheiner, S. *Acc. Chem. Res.* **1994**, *27*, 402−408.
(11) Filarowski, A.; Kochel, A.; Cieslik, K.; Koll, A. *J. Phys. Org. Chem.* **2005**, *18*, 1−8.
(12) Douhal, A. *Science* **1997**, *276*, 221−222.
(13) Smoluch, M.; Joshi, H.; Gerssen, A.; Gooijer, C.; van der Zwan, G. *J. Phys. Chem. A* **2005**, *109*, 535−541.
(14) Mukhopadhyay, M.; Banerjee, D.; Koll, A.; Mandal, A.; Filarowski, A.; Fitzmaurice, D.; Das, R.; Mukherjee, S. *J. Photochem. Photobiol. A: Chem.* **2005**, *175*, 94−99.
(15) Berbernan-Santos, M. N.; Choppinet, P.; Fedorov, A.; Jullien, L.; Valeur, B. *J. Am. Chem. Soc.* **2000**, *122*, 11876−11886.
(16) Douhal, A. *Acc. Chem. Res.* **2004**, *37*, 349−355.
(17) Tolbert, L. M.; Solntsev, K. M. *Acc. Chem. Res.* **2002**, *35*, 19−27.
(18) Douhal, A. *Chem. Rev.* **2004**, *104*, 1955−1976.
(19) Douhal, A.; Fiebig, T.; Chachisvilis, M.; Zewail, A. H. *J. Phys. Chem. A* **1998**, *102*, 1657−1660.
(20) Hansen, J. E.; Pines, E.; Fleming, G. R. *J. Phys. Chem.* **1992**, *96*, 6904−6910.
(21) Pastor, I.; Di Marino, A.; Mendicuti, F. *J. Phys. Chem. B* **2002**, *106*, 1995−2003.
(22) Douhal, A.; Amat-guerri, F.; Acuna, A. U. *Angew. Chem., Int. Engl.* **1997**, *36*, 1514−1516.
(23) Mondal, S. K.; Sahu, K.; Sen, P.; Roy, D.; Ghosh, S.; Bhattacharyya, K. *Chem. Phys. Lett.* **2005**, *412*, 228−234.
(24) Matsushita, Y.; Suzuki, T.; Ichimura, T.; Hikida, T. *J. Phys. Chem. A* **2004**, *108*, 7490−7496.
(25) Roberts, E. L.; Dey, J.; Warner, I. M. *J. Phys. Chem.* **1996**, *100*, 19681−19686.
(26) Cohen, B.; Huppert, D.; Solnstev, K. M.; Tsfadia, Y.; Nachliel, E.; Gutman, M. *J. Am. Chem. Soc.* **2002**, *124*, 7539−7547.
(27) Giestas, L.; Yihwa, C.; Lima, J. C.; Vautier-Giongo, C.; Lopes, A.; Macanita, A. L.; Quina, F. H. *J. Phys. Chem. A* **2003**, *107*, 3263−3269.
(28) Mukherjee, T. K.; Ahuja, P.; Koner, A. L.; Datta, A. *J. Phys. Chem. B* **2005**, *109*, 12567−12573.
(29) Park, J.; Datta, A.; Chowdhury, P. K.; Petrich, J. W. *Photochem. Photobiol.* **2001**, *73*, 105−109.

(30) Mukherjee, T. K.; Panda, D.; Datta, A. *J. Phys. Chem. B* **2005**, *109*, 18895−18901.
(31) Mukhopadhyay, M.; Banerjee, D.; Koll, A.; Filarowski, A.; Mukherjee, S. *Chem. Phys. Lett.* **2006**, *420*, 316−320.
(32) Mitra, S.; Tamai, N.; Mukherjee, S. *J. Photochem. Photobiol. A: Chem.* **2006**, *178*, 76−82.
(33) Das, R.; Mitra, S.; Mukherjee, S. *J. Photochem. Photobiol. A: Chem.* **1993**, *76*, 33−38.
(34) Mitra, S.; Das, R.; Mukherjee, S. *J. Photochem. Photobiol. A: Chem.* **1994**, *79*, 49−54.
(35) Das, R.; Mitra, S.; Nath, D.; Muherjee, S. *Indian J. Chem.* **1995**, *34 A*, 850−856.
(36) Das, R.; Mitra, S.; Mukherjee, S. *Chem. Phys. Lett.* **1994**, *221*, 368−372.
(37) Guha, D.; Mandal, A.; Das, R.; Mitra, S.; Mukherjee, S. *Isr. J. Chem.* **1999**, *39*, 375−385.
(38) Mitra, S.; Das, R.; Guha, D.; Mukherjee, S. *Spectrochim. Acta, Part A* **1998**, *54*, 1073−1081.
(39) Mandal, A.; Mitra, S.; Banerjee, D.; Bhattacharyya, S. P.; Mukherjee, S. *J. Chem. Phys.* **2003**, *118*, 3154−3160.
(40) Crampton, M. R.; Emokpae, T. A.; Howard, J. A. K.; Isanbor, C.; Mondal, R. *Org. Biomol. Chem.* **2003**, *1*, 1004−1011.
(41) Rahimipour, S.; Palivan, C.; Freeman, D.; Barbosa, F.; Fridkin, M.; Weiner, L.; Mazur, Y.; Gescheidt, G. *Photochem. Photobiol.* **2001**, *74*, 149−156.
(42) Maurady, A.; Zdanov, A.; de Moissac, D.; Beaudry, D. *J. Biol. Chem.* **2002**, *277*, 9474−9483.
(43) Kolbe, M.; Besir, H.; Essen, L O.; Oesterhelt, D. *Science* **2000**, *288*, 1390−1396.
(44) Organero, J. A.; Tormo, L.; Douhal, A. *Chem. Phys. Lett.* **2002**, *363*, 409−414.
(45) Cram, D. J. *Nature (London)* **1992**, *356*, 29−36.
(46) Organero, J. A.; Douhal, A. *Chem. Phys. Lett.* **2003**, *373*, 426−431.
(47) Friedberg, E. C. *Nature (London)* **2003**, *421*, 436−440.
(48) Chattopadhyay, N. *J. Photochem. Photobiol. A: Chem.* **1991**, *58*, 31−36.
(49) Yorozu, T.; Hoshino, M.; Imamura, M. *J. Phys. Chem.* **1982**, *86*, 4422−4426.
(50) Bi, S.; Ding, L.; Tian, Y.; Song, D.; Zhou, X.; Zhang, H. *J. Mol. Struct.* **2004**, *703*, 37−45.
(51) Kamlet, M. J.; Abboud, J. M.; Abraham, M. H.; Taft, R. W. *J. Org. Chem.* **1983**, *48*, 2877−2887.
(52) Eaton, D. F. *Tetrahedron* **1987**, *43*, 1551−1570.